

# The population of young stars in Orion A: X-rays and IR properties.



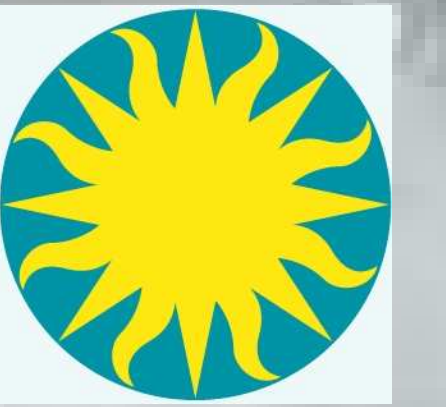
Ignazio Pillitteri<sup>1,\*</sup>, S. J. Wolk<sup>1</sup>, L. Allen<sup>2</sup>, S. T. Megeath<sup>3</sup>, R. A. Gutermuth<sup>1</sup> & *SOXS* collaboration.

<sup>1</sup> SAO-Harvard, 60 Garden St. Cambridge 02138 MA, USA

<sup>2</sup> National Optical Astronomy Observatory, USA

<sup>3</sup> Department of Physics & Astronomy, University of Toledo, OH, USA

\*email: ipillitteri@cfa.harvard.edu



## Introduction

Stars in the very early stages of their formation are characterized by strong IR excess and X-rays emission. We have observed the region of Orion A / L1641 in IR and X-ray bands with a program called *SOXS* obtained with *Spitzer* and *XMM-Newton* observatories. We aim to characterize the Young Stellar Objects (YSOs) population with the help of IR photometry from *2MASS* + *Spitzer* (IRAC & MIPS) and by means of X-rays fluxes, luminosities and plasma temperatures from *XMM-Newton* observations. The X-ray part of *SOXS* is composed by 7 *XMM-Newton* observations to which we have added 3 archive pointings. The maps below are the RGB mosaics of X-ray images of EPIC on board *XMM-Newton* and IR images of IRAC on board *Spitzer*. The upper crowded field is the archive Iota Ori observation, in which the bright O-type star in the center has a soft spectrum, due to shock interaction of stellar winds and thus it appears quite red. With the comparison of X-ray emission of stars in fields characterized by different levels (or absence) of UV flux from massive O-B we study the influence of the environment on the X-ray activity of very young Suns. We aim also to investigate the clustering of YSOs in the surveyed region (see Fig. 4).

## Pre Main Sequence Population.

Table 1: Number of PMS stars detected in *XMM-Newton* and with *Spitzer*/*2MASS* photometry.

Type	Protostars	CTTs	Trans. Disks	WTTs <sup>a</sup>	Total
X-rays det.	23	215	12	452	702
<i>Spitzer</i>	140	534	42	1130±53 <sup>b</sup>	1795 ÷ 1900
X-ray/IR	16%	40%	28%	40% <sup>c</sup>	~38%

<sup>a</sup> Weak T Tauri star candidates, i.e. stars with no IR excess.

<sup>b</sup> Poisson statistics.

<sup>c</sup> assume the same fraction of detection as PMS stars with disks (CTTs), see comment below.

Through *Spitzer* and *XMM-Newton* we identify ~702 PMS stars that emit in X-rays out of 1060 X-ray sources. By assuming the same fraction of X-ray detection of WTT stars and CTT stars we estimate a population of ~1850 PMS stars, for an overall detection efficiency of ~38% among PMS stars and a mean density of PMS stars of ~750 stars deg<sup>-2</sup>. Our sensitivity limit is  $L_X \sim 5 \cdot 10^{28}$  erg s<sup>-1</sup>. By using COUP data as template, we estimate that we have completeness of WTTs sample above  $L_X \sim 10^{29.3}$  erg s<sup>-1</sup> but that a fraction > 50% could be undetected below  $10^{29.3}$  erg s<sup>-1</sup>, at masses  $\leq 0.8 - 1M_\odot$ . We observe also that the fraction of X-rays detected *Transition Disk* objects (see fig. 1) is ~28%, thus lower than that of X-ray detected CTT stars. This fraction strongly supports the guess that the population of low mass WTTs missed in X-rays is above 50%. By using a fork of 30%–50% of X-ray detected WTTs, we bracket the total population of PMS stars in this region to be between 1500 and 2130 stars with masses of a few solar masses to the limit of Brown Dwarfs, a population larger than the one embedded in the Orion Nebula Cloud. As complement to this study, our team is carrying also an optical follow up with spectroscopy to better characterize true WTTs and to distinguish them from field stars.

## X-ray luminosities.

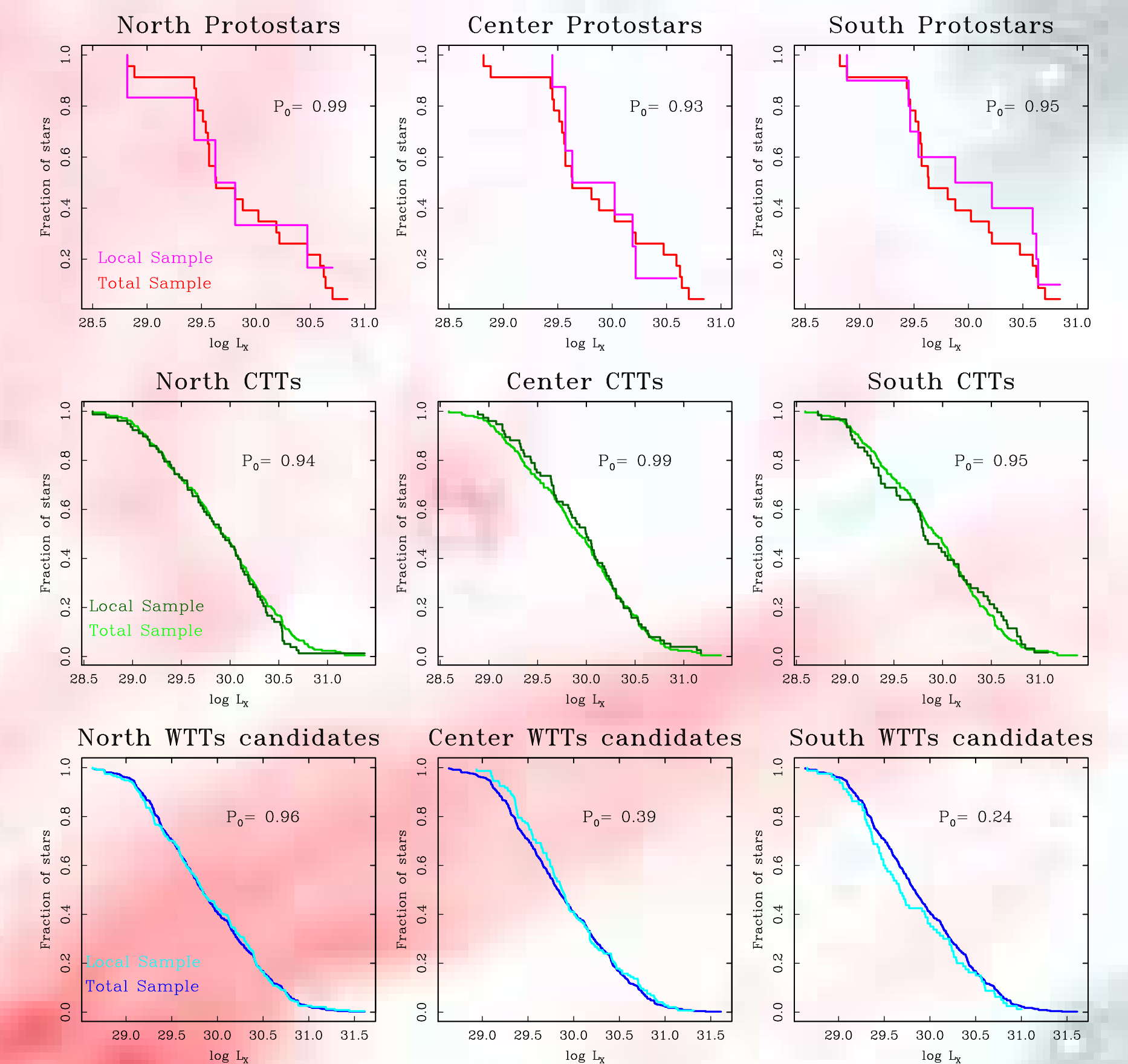


Fig. 2: X-ray luminosity distributions for Protostars, CTTs, and WTTs candidates for North, Center and South part of the survey. KS test null probabilities between total and local samples are indicated in the plots. Differences in WTTs luminosities are found in the Center zone with respect to North and South zones.

Table 2: KS test null probabilities for differences between Protostars, CTTs and WTTs candidates of different zones. Differences are suggested in the  $L_X$  distributions of WTTs candidates of different zones. Second part of the Table lists the medians and  $1\sigma$  ranges of  $L_X$  for each sample and by zones.

Type/Zone	North—Center	North—South	Center—South
Protostars	0.84	0.89	0.82
CTTs/Disks	0.95	0.46	0.62
WTTs cand.	0.11	0.27	0.06
$\langle L_X \rangle$	North	Center	South
Protostars	29.73 (29.36-30.53)	29.87 (29.57-30.21)	30.08 (29.46-30.63)
CTTs/Disks	29.92 (29.28-30.42)	30.00 (29.35-30.46)	29.80 (29.21-30.61)
WTTs cand.	29.84 (29.22-30.51)	29.87 (29.37-30.53)	29.67 (29.26-30.45)

## IR photometry.

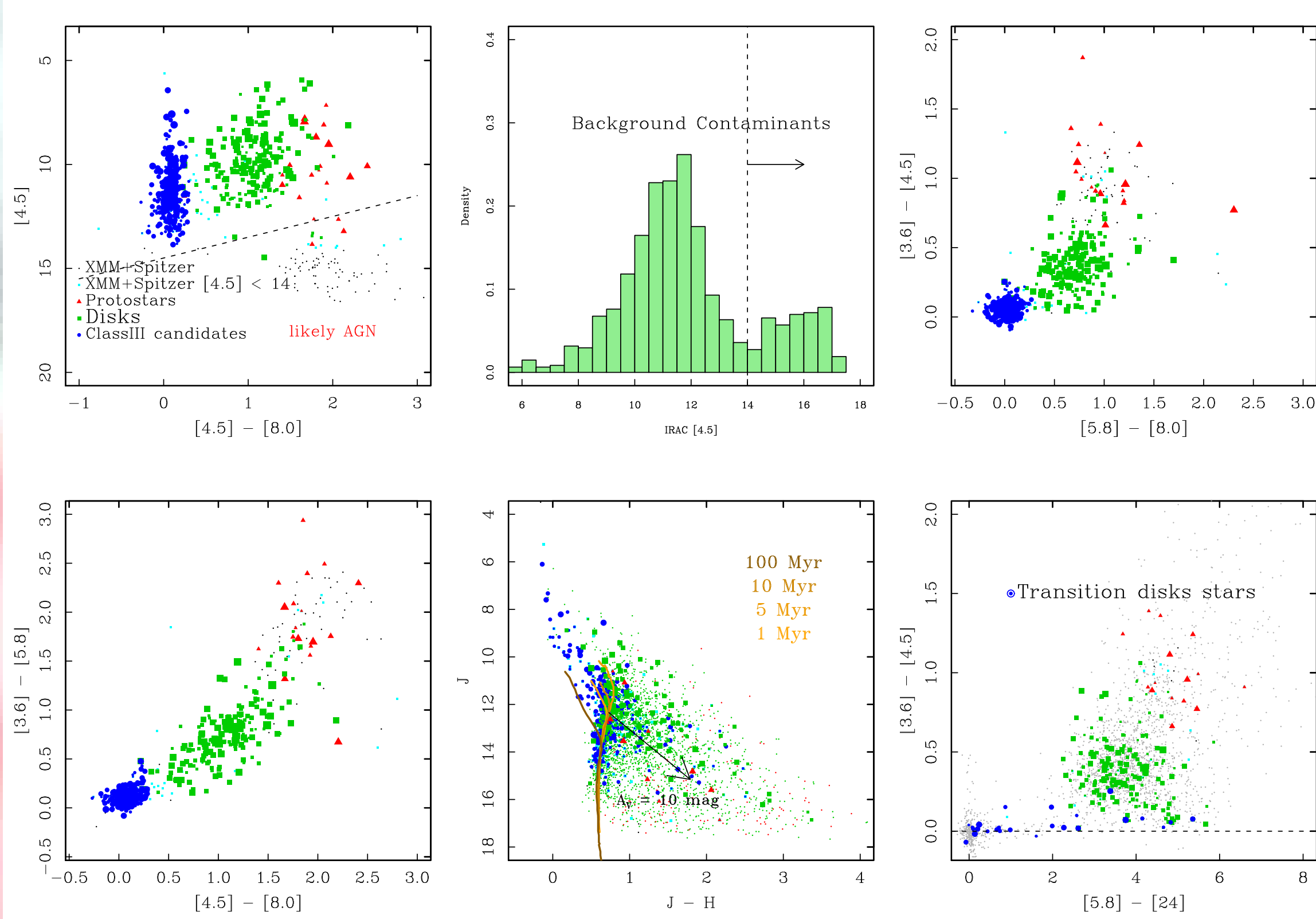


Fig. 1: IRAC and 2MASS photometry of the counterparts to X-ray sources. Symbol sizes are proportional to X-ray luminosities, colors code the samples as follows:

- red: protostars (IR excess, Class 0/I YSOs)
- green: CTTs with disks (IR excess, Class II YSOs)
- blue: WTTs candidates (X-ray detection, no IR excess, Class III YSOs)
- black: faint objects, IRAC [4.5] > 14 mag
- cyan: unclassified objects with [4.5] < 14 mag.

*Spitzer* photometry allows a crisp classification between WTTs candidates, CTTs, Protostars, and to isolate likely distant AGNs. We detected 12 *Transition disk* objects (blue circles) in X-rays: they are recognized by a large excess in the 24 $\mu$ m band but almost no IR excess in IRAC bands. 2MASS diagram shows that stellar ages are mostly comprised between 1 and 10 Myr.

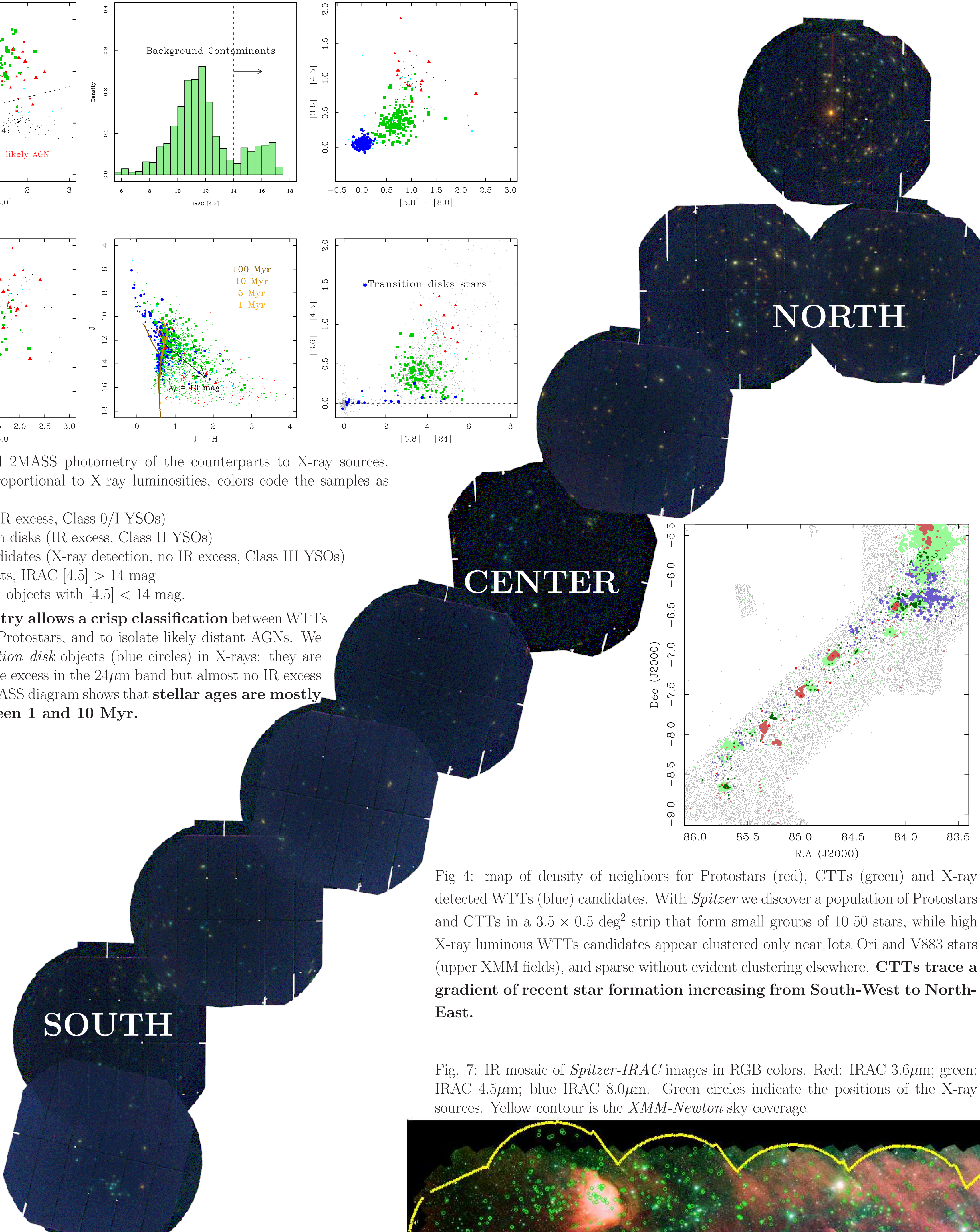


Fig. 4: map of density of neighbors for Protostars (red), CTTs (green) and X-ray detected WTTs (blue) candidates. With *Spitzer* we discover a population of Protostars and CTTs in a  $3.5 \times 0.5$  deg<sup>2</sup> strip that form small groups of 10-50 stars, while high X-ray luminous WTTs candidates appear clustered only near Iota Ori and V883 stars (upper XMM fields), and sparse without evident clustering elsewhere. CTTs trace a gradient of recent star formation increasing from South-West to North-East.

Fig. 7: IR mosaic of *Spitzer*-IRAC images in RGB colors. Red: IRAC 3.6 $\mu$ m; green: IRAC 4.5 $\mu$ m; blue IRAC 8.0 $\mu$ m. Green circles indicate the positions of the X-ray sources. Yellow contour is the *XMM-Newton* sky coverage.

Fig. 6: X-ray mosaic of *XMM-EPIC* images in RGB colors. Red: 0.3-1.0 keV; green: 1.0-2.5 keV; blue: 2.5-8.0 keV. X-ray images are normalized by effective area and vignetting factor, smoothed and displayed on a power-law scale.

## Analysis of X-ray spectra.

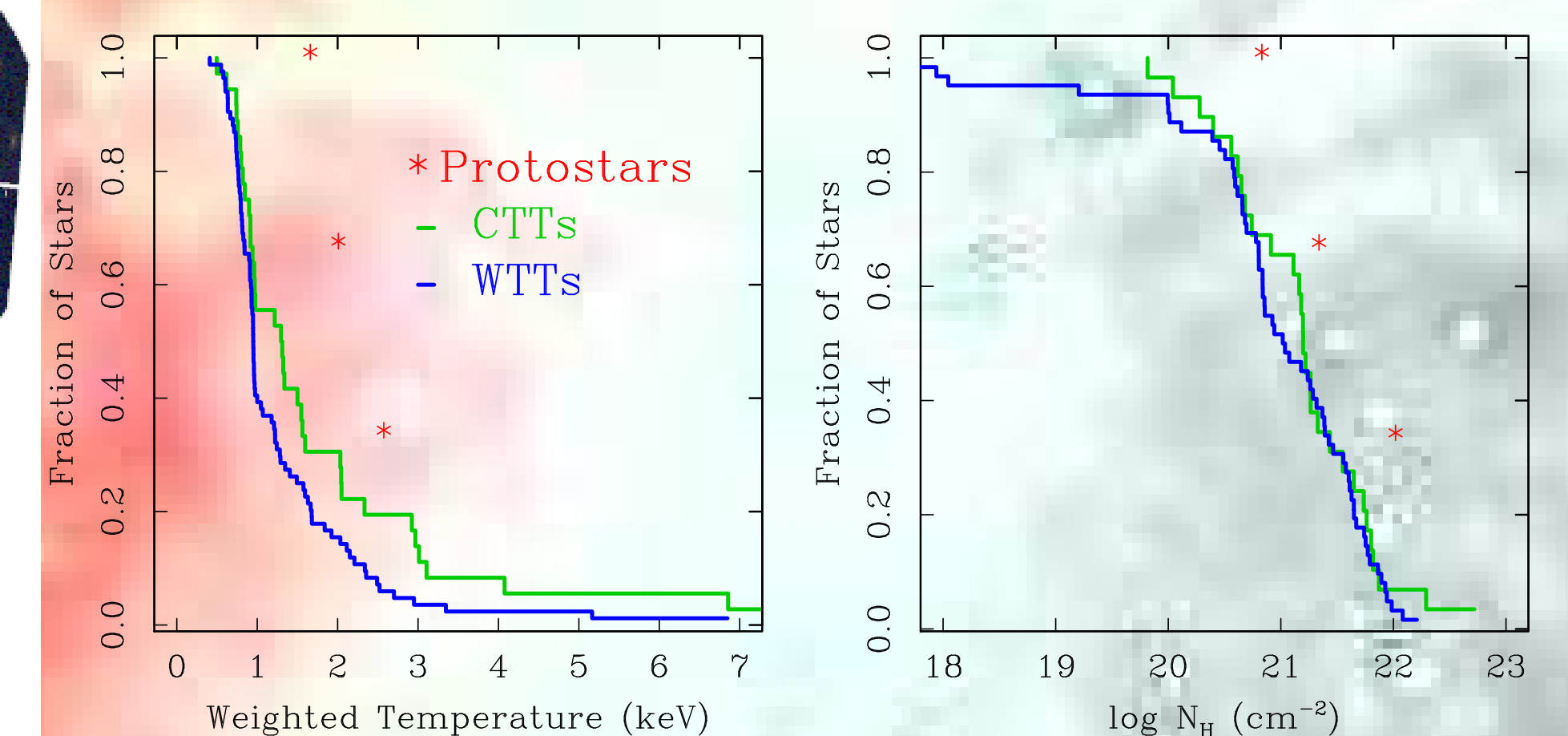


Fig. 3: Protostars have higher  $\langle kT \rangle$  and  $N_H$  with respect to CTTs which in turns appear hotter than WTTs. High  $\langle kT \rangle$  values in Protostars are due to stronger absorption and/or intrinsic hotter plasma than in CTTs and WTTs.

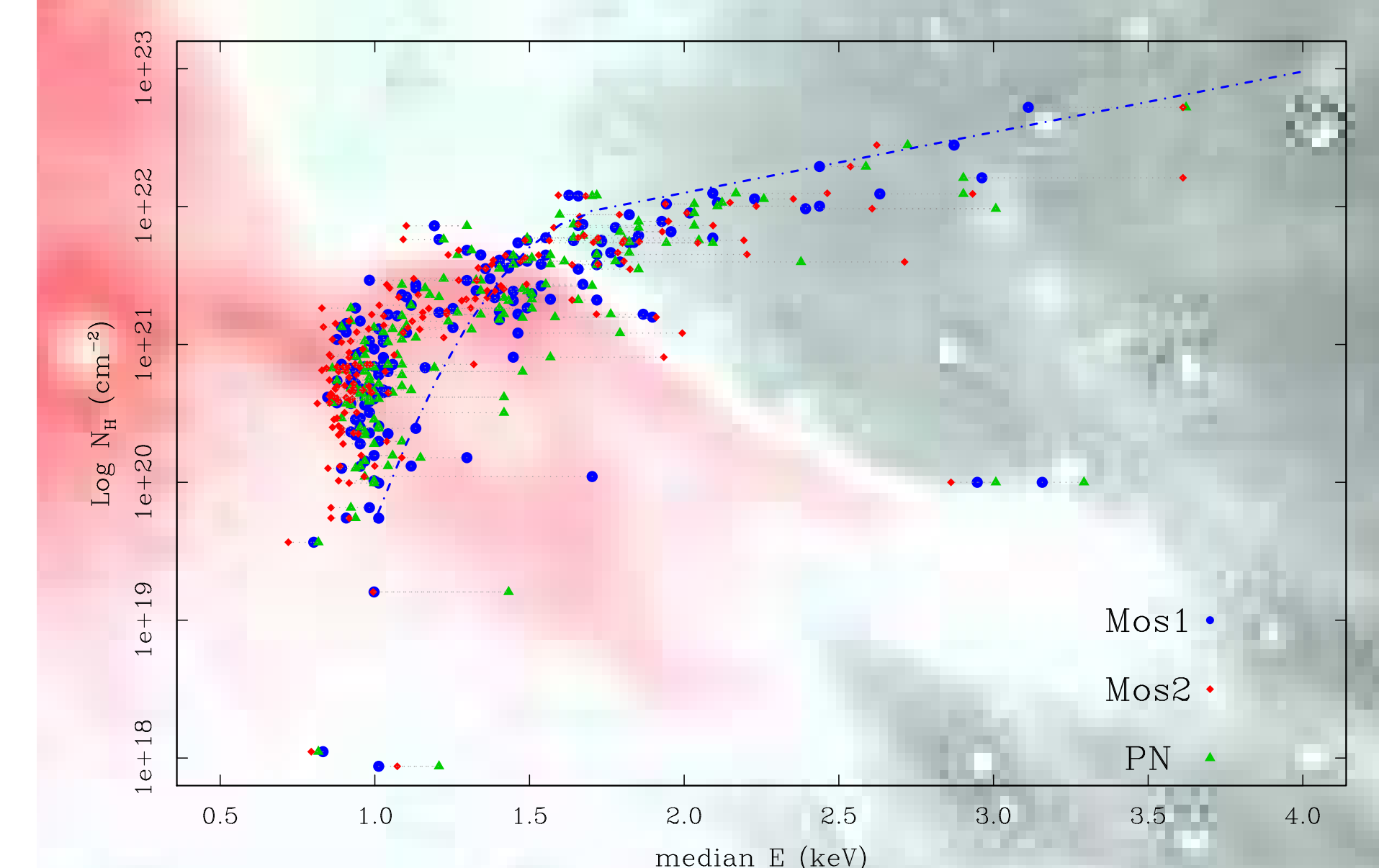


Fig. 5: as in Feigelson et al. (2005) for COUP data, we find a coarse correlation between median energy of X-ray spectra of *SOXS* sources and  $N_H$  column absorption (from spectral fits). For energies above  $kT \sim 1.5$  keV, EPIC-XMM is in agreement with *Chandra-ACIS*, while below 1.5 keV *XMM-EPIC* has a steeper response than *Chandra-ACIS*.

